The EMBO Journal vol.14 no.22 pp.5532–5541, 1995

C-terminus determinants for Mg^{2+} and polyamine block of the inward rectifier K^+ channel IRK1

Maurizio Taglialatela[1,2], Eckhard Ficker, Barbara A.Wible and Arthur M.Brown

Rammelkamp Center for Research, MetroHealth Campus, Case Western University, 2500 MetroHealth Drive, Cleveland, OH 44109-1998, USA and [1]Department of Neuroscience—Section of Pharmacology, 2nd School of Medicine, University of Naples 'Federico II', 5 Via S.Pansini, 80131 Naples, Italy

[2]Corresponding author

Critical loci for ion conduction in inward rectifier K^+ channels are only now being discovered. The C-terminal region of IRK1 plays a crucial role in Mg_i^{2+} blockade and single-channel K^+ conductance. A negatively charged aspartate in the putative second transmembrane domain (position 172) is essential for time-dependent block by the cytoplasmic polyamines spermine and spermidine. We have now localized the C-terminus effect in IRK1 to a single, negatively charged residue (E224). Mutation of E224 to G, Q and S drastically reduced rectification. Furthermore, the IRK1 E224G mutation decreased block by Mg_i^{2+} and spermidine and, like the E224Q mutation, caused a dramatic reduction in the apparent single-channel K^+ conductance. The double mutation IRK1 D172N+ E224G was markedly insensitive to spermidine block, displaying an affinity similar to ROMK1. The results are compatible with a model in which the negatively charged residue at position 224, E224, is a major determinant of pore properties in IRK1. By means of a specific interaction with the negatively charged residue at position 172, D172, E224 contributes to the formation of the binding pocket for Mg^{2+} and polyamines, a characteristic of strong inward rectifiers.
Keywords: inwardly rectifying K^+ channels/Mg^{2+} block/ polyamines block/potassium conductance

Introduction

Inwardly rectifying K^+ channels (IRKs) maintain resting membrane potential and permit prolonged depolarization like those occurring during the cardiac action potential (Hille, 1992). Inward rectification in IRKs has been attributed to both fast blockade of the pore by internal Mg^{2+} and/or a slow 'intrinsic' gating process (Matsuda *et al.*, 1987; Vandenberg, 1987; Ishihara *et al.*, 1989; Silver and DeCoursey, 1990). In cloned IRKs, intrinsic gating has recently been shown to depend on pore blockade by cytoplasmic polyamines (PAs), particularly spermidine (SPD) and spermine (SPM) (Fakler *et al.*, 1994, 1995; Ficker *et al.*, 1994; Lopatin *et al.*, 1994).

For cloned IRKs, current topological models predict two potential transmembrane domains called M_1 and M_2 separated by an H_5 region having extensive sequence similarity with a conserved H_5 region which is thought to line the ion conduction pathway of voltage-dependent K^+, Na^+, Ca^{2+} and cyclic nucleotide-gated channels. A single, negatively charged residue located in the putative second transmembrane domain of IRK1 (Kubo *et al.*, 1993a) (an aspartate at position 172) controls the gating phenotype (Stanfield *et al.*, 1994; Wible *et al.*, 1994) as a major contributor to the high affinity PA binding site (Ficker *et al.*, 1994). In fact, mutation of the M_2 aspartate in the strong rectifier IRK1 to an asparagine, the corresponding residue in ROMK1 (Ho *et al.*, 1993), a weakly rectifying and time-independent channel, removed time-dependent gating. The reverse mutation in ROMK1 (N171D) produced time-dependent gating very similar to IRK1 (Wible *et al.*, 1994). Although time-dependent gating seems to be specifically conferred by the Asp in M_2, PA block was much stronger in IRK1 D172N than in wild type ROMK1. This result suggests that additional sites might contribute to PA binding in IRK1 (Ficker *et al.*, 1994). Since the molecular determinants for Mg_i^{2+} binding and K^+ conduction in IRK1 had been shown to be specified by the C-terminus (Taglialatela *et al.*, 1994), it seemed possible that the additional PA site might be in this region. The aim of the present study was to localize further the Mg_i^{2+} and PA binding sites within the C-terminus, thereby specifying the composition of the IRK1 pore more precisely.

Results

Localizing the C-terminal segment producing inward rectification in IRK1

Large-scale chimeric constructs between the two IRKs, IRK1 and ROMK1, have provided evidence that the IRK1 C-terminus contains molecular determinants for strong inward rectification (Taglialatela *et al.*, 1994). In fact, the substitution of the IRK1 C-terminal tail with the corresponding ROMK1 segment generated a channel which was strongly rectifying when expressed in *Xenopus* oocytes (CHM C, Figure 1), while the reverse construct (REV. CHM C) failed to express functional channels. The C-terminus of IRK1 is 250 amino acids long, comprising more than half of the deduced amino acid sequence of the channel (428 amino acids). We have engineered several chimeric channels (Figure 2B) in which the substituted IRK1 C-terminal segment is progressively shorter, in order to locate the region producing rectification more precisely. The C-terminus has been divided into five segments: C_1, C_2, C_3, C_4 and C_5. This segmentation has been chosen on the basis of the results of the hydropathy plot shown in Figure 2A, which suggests the presence of two hydrophobic stretches (C_2 and C_4) which could be membrane associated. C_1 is a 72 residue spacer; C_3 is a charged stretch between C_2 and C_4; C_5 is the last segment. The

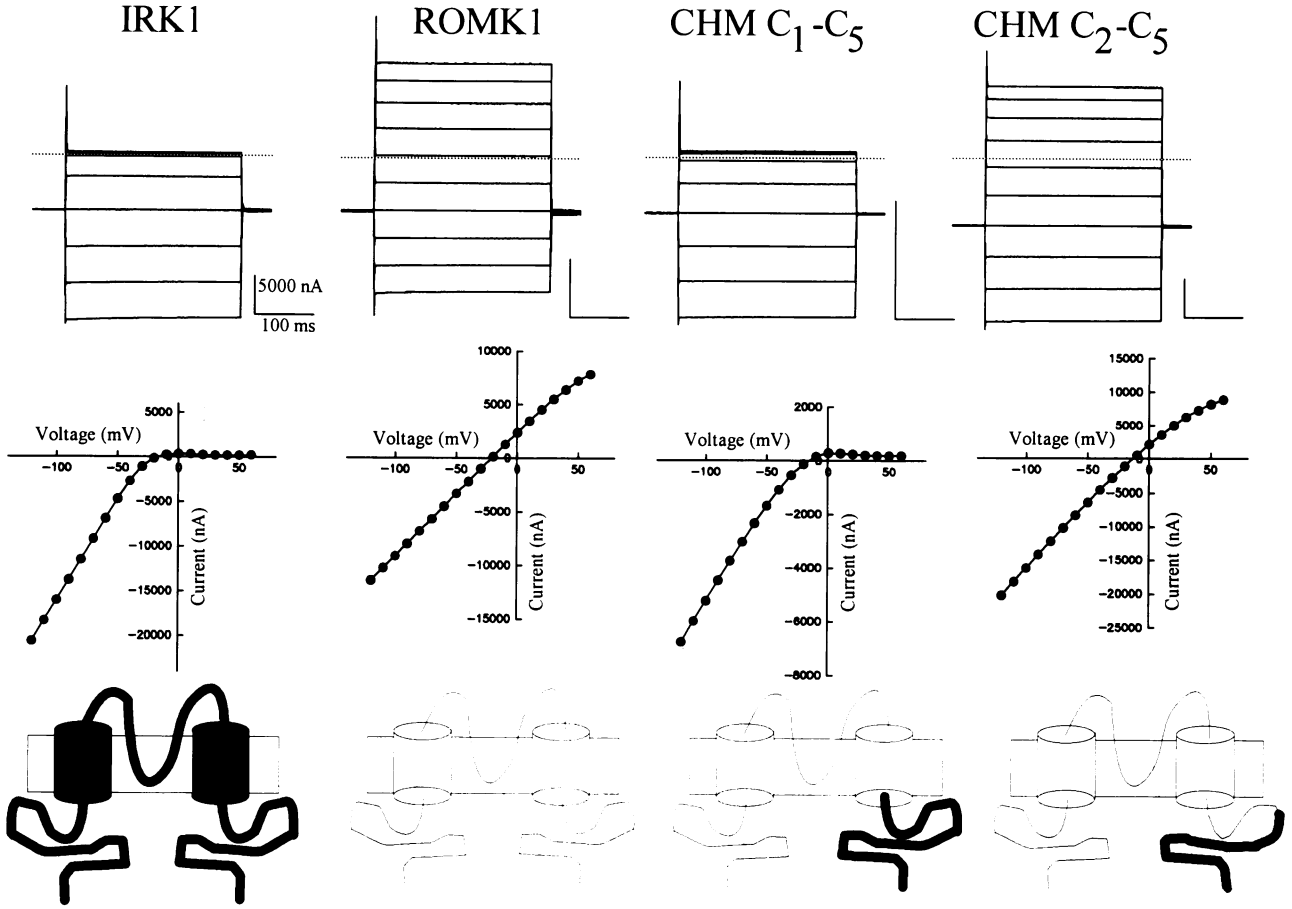

Fig. 1. Macroscopic currents recorded from oocytes injected with ROMK1, IRK1 and the ROMK1/IRK1 chimeric constructs CHM C_1–C_5 and C_2–C_5. Macroscopic current from cRNA injected *Xenopus* oocytes was recorded with conventional two-microelectrode voltage-clamp techniques. Holding potential: –60 mV; 250 ms steps from –120 mV to +60 mV in 20 mV increments; return potential: –60 mV. Dashed lines indicate zero current. Bath solution was high K^+-MES. In the bottom panels, the relationship of the steady-state current (measured at the end of the depolarizing pulses) to voltage is shown. The data were not corrected for a –15 mV zero-current offset, probably resulting from a MES,Cl liquid junction potential.

amino acids at which chimeric junctions were made were: N251 for the C_1–C_2, H271 for the C_2–C_3, E293 for the C_3–C_4, and Q310 for the C_4–C_5 junctions.

Figure 1 shows macroscopic currents recorded with two-microelectrode voltage-clamp from *Xenopus* oocytes expressing the ROMK1/IRK1 C_2–C_5 chimeric channel compared with those of IRK1, ROMK1 and CHM C (also called ROMK1/IRK1 C_1–C_5 CHM). The strong rectification of the C_1–C_5 chimera is completely removed by restricting the replaced segment onto ROMK1 to the C_2–C_5 region. This suggests that determinants in the C_1 region of IRK1, which is 72 amino acids long (about one-fourth of the entire C-terminus) are responsible for the strong inward rectification of the C_1–C_5 chimera. This conclusion was also strengthened by the weak rectification observed in the only other expressing construct, the C_4–C_5 CHM (Figure 2B).

Nature of the rectification conferred by the C_1 region

The strong inward rectification of the C_1–C_5 CHM channel is due to pore blockade by internal cations (Table I). This channel displays a high affinity for both internal Mg^{2+} and SPD (Figure 3); by contrast, the presence of the ROMK1 C_1 segment in the ROMK1/IRK1 C_2–C_5 CHM channel abolished the sensitivity to SPD (Figure 3), resembling very closely the wild type ROMK1 channels (Ficker *et al.*, 1994). It is also important to underline that the C_1–C_5, the C_2–C_5 and the C_4–C_5 CHM channels displayed instantaneous rectification, presumably due to the presence of a non-charged asparagine residue at position 171 (Stanfield *et al.*, 1994; Wible *et al.*, 1994). In addition, as shown in Figure 3, SPD block of the CHM C_1–C_5 channel is completely time-independent, suggesting fast rates of interaction of the blocker with the C_1 sites. In this regard, SPD had similar intrinsic affinity and blocking kinetics in the CHM C_1–C_5 channels as in the IRK1 D172N channels (Ficker *et al.*, 1994).

A single negatively charged residue in C_1 is crucial for inward rectification

Alignment of the C_1 sequence between IRK1 and ROMK1 shows that there are only four positions (E191, D205, E224 and D249) which are occupied by negatively charged amino acids in IRK1 and either neutralized (G204, G223, N248) or substituted with residues of opposite charge (K190) in ROMK1 (Figure 4A). We therefore introduced the corresponding ROMK1 residue at each of these four positions in IRK1 (IRK1 E191K, IRK1 D205G, IRK1 E224G, IRK1 D249N), in order to investigate whether

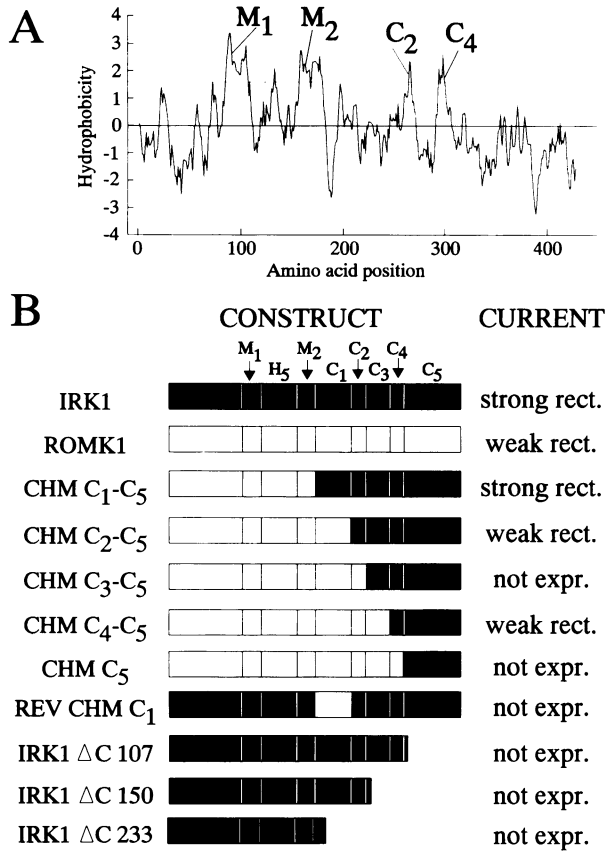

Fig. 2. Hydropathy profile of IRK1 and design of the ROMK1/IRK1 chimeric constructs. (**A**) Hydropathy profile of IRK1. The hydrophobicity values were calculated according to Kyte and Doolittle (1982). In order to emphasize the presence of possible membrane-associated segments in the C-terminal region, a window of nine amino acids was used, instead of the classical 19 amino acids for predicting transmembrane domains. The putative transmembrane segments M_1 and M_2, as well as the two membrane-associated regions in the C-terminus, C_2 and C_4, are indicated. (**B**) ROMK1/IRK1 chimeric constructs and IRK1 deletion design and functional results obtained. 'Strong rect.' or 'Weak rect.' stand for strong or weak rectification of the expressed channels; rectification ratios of the current 60 mV above or below the reversal potential were >0.5 for weakly rectifying channels and <0.2 for strongly rectifying channels. 'Not expr.' denotes constructs not giving rise to functional channels. Non-expressed constructs were those giving rise to macroscopic currents, at −120 mV, <200 nA in whole-cell recordings (at least four oocytes from two separate batches); currents smaller than this value are indistinguishable from those present in non-injected oocytes.

any of those residues were responsible for the differences in rectification conferred by the IRK1 C_1 region.

Figure 4B shows macroscopic currents recorded with two-microelectrode voltage-clamp from *Xenopus* oocytes injected with the cRNA encoding each of these mutants, compared with those expressed by IRK1. The results show that, while no major effect was observed on macroscopic current rectification and kinetics by the mutations IRK1 E191K, IRK1 D205G and IRK1 D249N, the mutant IRK1 E224G clearly displayed reduced rectification together with slower, time-dependent kinetics in both outward as well as inward currents. In order to achieve better time resolution, we applied the macropatch technique to study the macroscopic currents from the IRK1 E224G mutant (Figure 5; see also Figure 9); the prominent outward currents and the slow, time-dependent inward currents were more clearly resolved.

Table I. Mg^{2+} and SPD block in IRKs

Channel	Mg^{2+} affinity (K_d at +40 mV)[a]	SPD affinity (K_d at +40 mV)[a]
IRK1	17 μM[b]	18 nM[d]
ROMK1	1.7 mM[b]	2.2 mM[d]
C_1–C_5 CHM	90 μM[b]	3 μM
C_2–C_5 CHM	>1 mM	>1 mM
IRK1 D172N	30 μM[c]	446 nM[d]
IRK1 E224G	180 μM	6 μM
IRK1 D172N+E224G	N.D.	>500 μM
IRK1 D172N+E224Q	N.D.	>500 μM

[a]K_d values were calculated by fitting the cuurent values at varous blocker concentration to the following binding isotherm: $y = max/(1 + X/K_d)n$, where X is the blocker concentration and n the Hill coefficient. The fitted values for n were between 0.8 and 1.2.
[b]Data taken from Taglialatela *et al.* (1994).
[c]Data taken from Wible *et al.* (1994).
[d]Data taken from Ficker *et al.* (1994).

To determine whether these kinetic changes were produced by the reduced volume and increased flexibility of the protein consequent to the introduction of the glycine residue at this position, we generated a more conservative mutant in which the negative charge of the glutamate residue was neutralized by a glutamine substitution (IRK1 E224Q), as well as an IRK1 E224S mutant, since an S is present at a corresponding position in the G-protein gated IRK (GIRK1) (Dascal *et al.*, 1993; Kubo *et al.*, 1993b). Both mutants displayed prominent gating in both inward and outward currents (Figure 5), although the time constants for outward current inactivation were clearly faster in the E224G mutant than in the E224Q or E224S mutants. Collectively, the fact that the E224Q and E224S mutations produce qualitatively similar changes to those described for the E224G mutation suggests that it is the presence of the negative charge at this position, rather than the absence of the glycine, that determines the rectification properties of IRK1.

At 1 kHz recording bandwidth, dramatic changes introduced by the mutation at position 224 in IRK1 were also recorded at the single channel level (Figure 6). The apparent single channel K^+ conductance and kinetics of IRK1 were dramatically altered by the E224G mutation: the open channel displayed a flickery appearance with a marked increase in the open channel noise. These changes were even more apparent in the E224Q mutation, in which the estimation of the conductance was prevented by the noisy appearance of the single channel openings. IRK1 single channel currents were, instead, characterized by very slow kinetics and no detectable increase in open channel noise. Even when the cutoff filter was set at 2 kHz, the flickerings of the single channel openings were not fully resolved (data not shown).

We asked next whether we could modify the pore properties and increase rectification in ROMK1 by introducing a single negative charge at the corresponding position in C_1. The ROMK1 G223E mutant was examined at both macroscopic and single channel level (Figure 7). This mutant displayed rectification and single channel properties identical to wild type ROMK1: weak rectification of the macroscopic currents (consistent with weak block of the open channel by internal Mg^{2+} and SPD), large single channel K^+ conductance and relatively faster

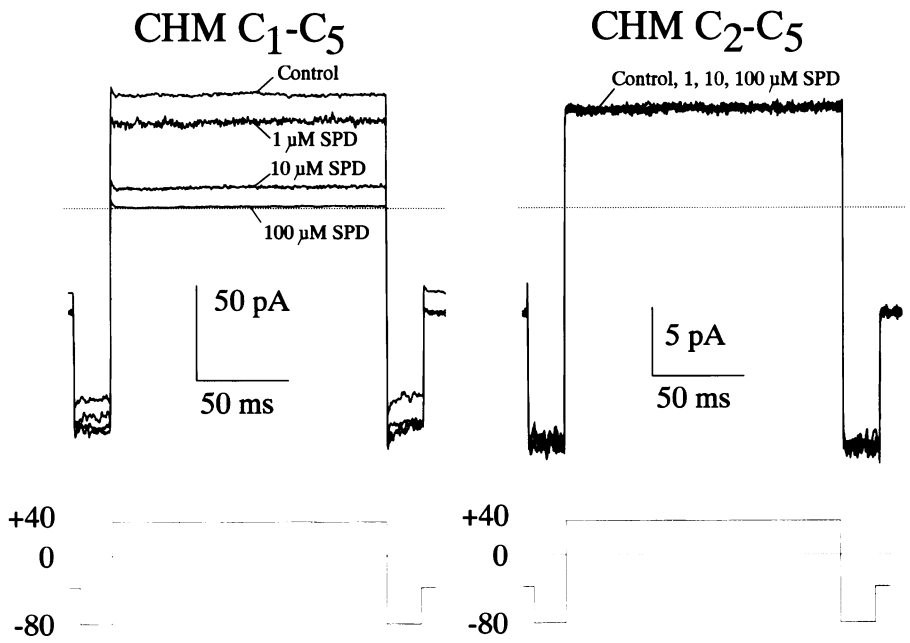

Fig. 3. Effect of SPD on the ROMK1/IRK1 CHM constructs C_1–C_5 and C_2–C_5. Averaged single-channel records recorded in the inside-out configuration in control solution and after patch exposure to increasing SPD concentrations (1, 10 and 100 μM). Test potential: +40 mV. Hyperpolarizing pre- and post-pulses: –80 mV. As judged from the maximal current obtained, the recording shown in the left panel (C_1–C_5 CHM) was obtained from a patch containing ~50–100 channels, while the one on the right panel (C_2–C_5 CHM) contained 5–10 channels. Pipette and bath solutions were K^+-Ringer and iso-K^+ respectively.

single channel kinetics when compared with IRK1. The fact that the C_1 region can confer strong rectification upon ROMK1, as suggested by the C_1–C_5 CHM/C_2–C_5 CHM results, but that the G223E mutation in ROMK1 did not increase rectification, seems to suggest that the overall tridimensional architecture of the C_1 region might be different between ROMK1 and IRK1 channels, despite rather marked similarities of their hydropathy plots (data not shown for ROMK1). The relatively minor role played by the C-terminus in specifying ROMK1 pore properties is also suggested by the fact that another position, residue 171, appears to be a major determinant for Mg_i^{2+} and PA blockade. The ROMK1 N171D mutant increased Mg_i^{2+} affinity by ~10-fold (Lu and MacKinnon, 1994; Wible *et al.*, 1994) and SPD affinity by ~10^4-fold (Ficker *et al.*, 1994; Lopatin *et al.*, 1994), whereas the IRK1 D172N mutation only accounts for a 20-fold difference in SPD affinity, with no change in Mg_i^{2+} blocking rates (Wible *et al.*, 1994). Also in a recently cloned IRK from the rat brain, BIR10, the substitution of the corresponding negatively charged M_2 position with an asparagine (mutation BIR10 E158N) caused a loss by as much as five orders of magnitude of sensitivity to SPM (Fakler *et al.*, 1994).

Mechanism of decreased inward rectification in IRK1 E224 mutants

We next examined the effect of neutralization of the negative charge at position 224 in IRK1 on internal Mg^{2+} and PA block (Table I). Figure 8A shows that in the IRK1 E224G mutant, as already demonstrated for IRK1, excision of the patch in the inside-out configuration in the absence of internal Mg^{2+} and PAs removed most of the rectification, even though a slight inward rectification of the open channel still persisted. After achieving the inside-out configuration, the addition of 288 μM internal Mg^{2+} to the IRK1 E224G channels resulted in an apparent slow inactivation of the outward currents due to slow entry into the channel (ON rate). The same concentration of Mg^{2+} has already been shown to completely block the outward currents in IRK1 (Taglialatela *et al.*, 1994; Wible *et al.*, 1994). Furthermore, the ON rate for Mg_i^{2+} in IRK1 was virtually instantaneous and no apparent inactivation of the outward current could be detected (Ficker *et al.*, 1994). In IRK1 E224G, the exit from the blocked channel (OFF rate) of Mg^{2+}, which is virtually instantaneous in IRK1, is greatly slowed, leading to time-dependent macroscopic current activation upon hyperpolarization (Figure 8A). The more dramatic effect of the mutation on the ON than on the OFF rate for internal Mg^{2+} leads to a 10-fold decrease in the channel intrinsic Mg^{2+} affinity, the K_d at +40 mV being 180 μM.

A more dramatic effect exerted by the IRK1 E224G mutation was observed on SPD binding. At +40 mV, the SPD affinity was decreased by ~300-fold, as shown in Figure 8B. One micromolar SPD, which almost completely abolished IRK1 currents, only slightly affected IRK1 E224G currents; the kinetics of the ON rate were clearly slower in the mutant when compared with the wild-type kinetics. These results suggest that in IRK1, position 224 is an important determinant for both Mg^{2+} and PA binding, and the decreased rectification of the E224 mutants is due to a decrease in affinity of the channel for these internal cations.

Having identified position 224 as an important determinant for internal cation binding in IRK1, we engineered a double mutant (IRK1 D172N+E224G), in which the previously identified site in M_2 had also been neutralized. Figure 9A shows macropatch currents obtained from IRK1

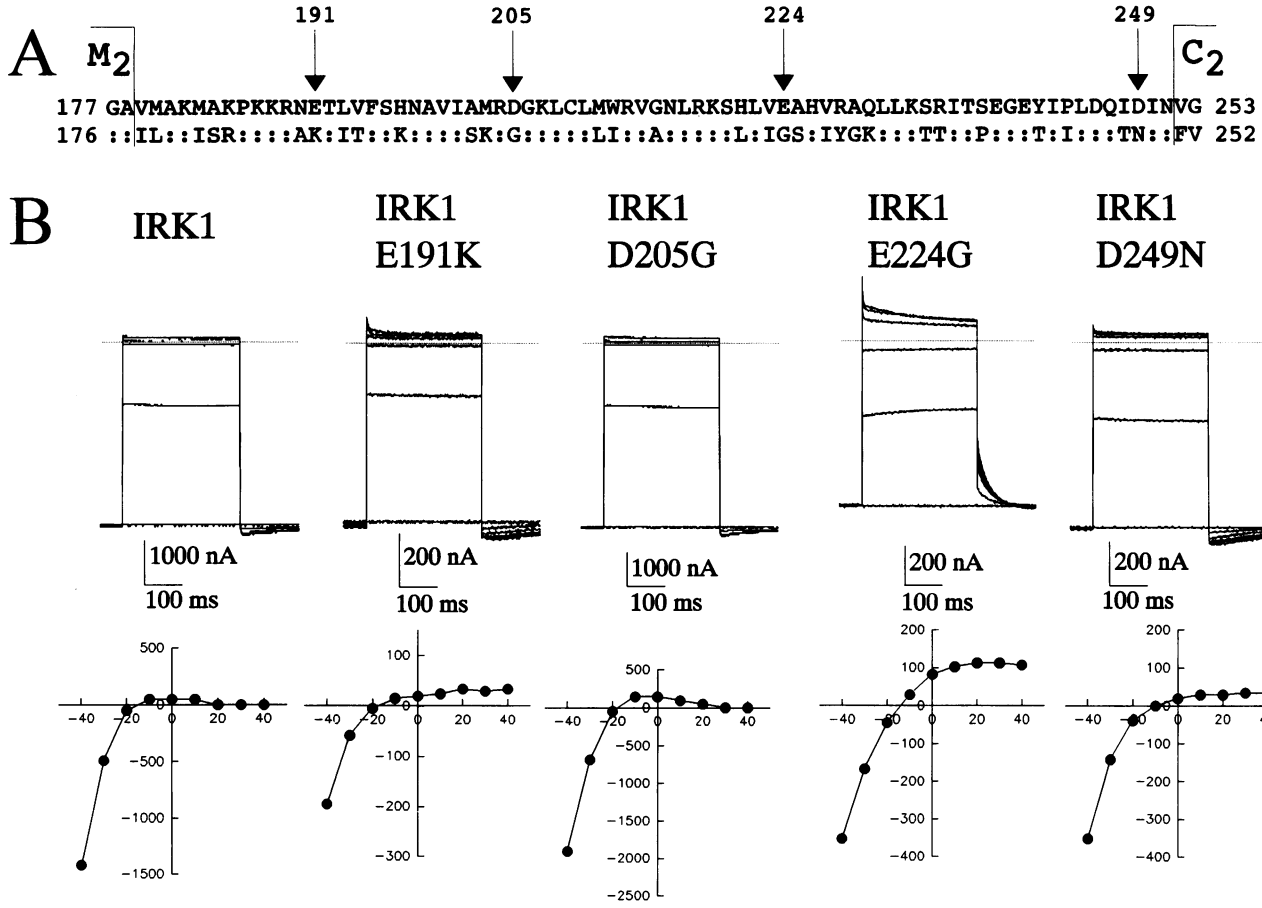

Fig. 4. Alignment of the C_1 amino acid sequences of IRK1 and ROMK1 and effect of the non-conserved charge substitutions. (**A**) Alignment of the IRK1 and ROMK1 amino acid sequences in the C_1 region. The non-conserved negative charges in IRK1 (E191, D205, E224 and D249) are marked with an arrow. (**B**) Two-microelectrode voltage-clamp recordings from *Xenopus* oocytes injected with cRNAs encoding IRK1 or its mutations E191K, D205G, E224G and D249N. Holding potential: –60 mV; 250 ms steps from –120 mV to +40 mV in 20 mV increments; return potential: –60 mV. Dashed lines indicate zero current. Bath solution was high K^+-MES. In the bottom panels, the relationship of the steady-state current (measured at the end of the depolarizing pulses) to the indicated voltages is shown. The data were not corrected for a –15 mV zero-current offset, probably resulting from a MES,Cl liquid junction potential.

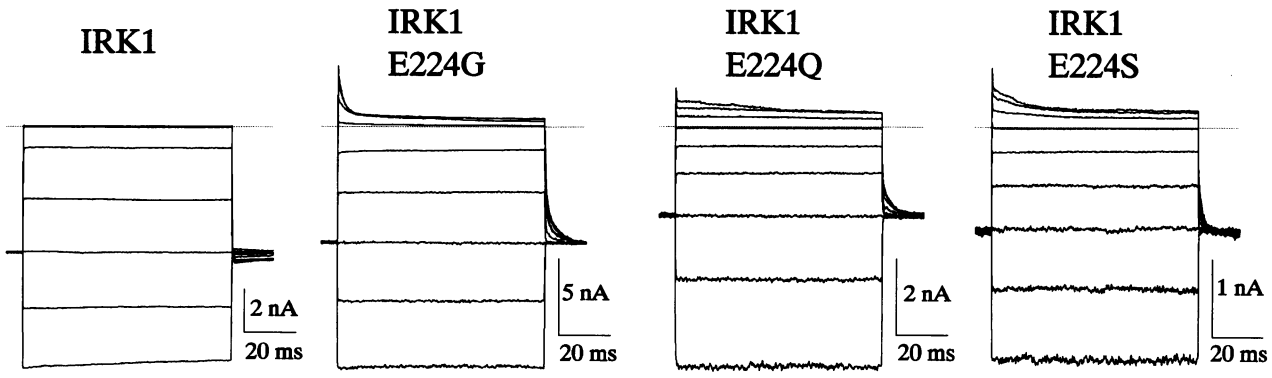

Fig. 5. Macroscopic gating in IRK1 E224 mutants. Unsubtracted cell-attached macropatch recordings from *Xenopus* oocytes injected with IRK1, IRK1 E224G, IRK1 E224Q, or IRK1 E224S mRNAs. Holding potential: –60 mV. Test pulses from –100 mV to +60 mV, in 20 mV steps; return potential: –60 mV. Pipette and bath solutions were K^+-Ringer and iso-K^+ respectively.

mutants D205G, E224G and D172N+E224G. As already introduced, the D205G mutant displayed wild-type kinetics, while the E224G currents activated very slowly upon hyperpolarization. As in the case of the D172N mutant alone, the double mutant D172N+E224G displayed time-independent kinetics (Wible *et al.*, 1994). Furthermore, even in Mg^{2+}- and PA-free inside-out configuration, the D172N+E224G mutant channel was still markedly rectifying (Figure 9B); it is likely that this results from a reduced ability of the internal mouth of the

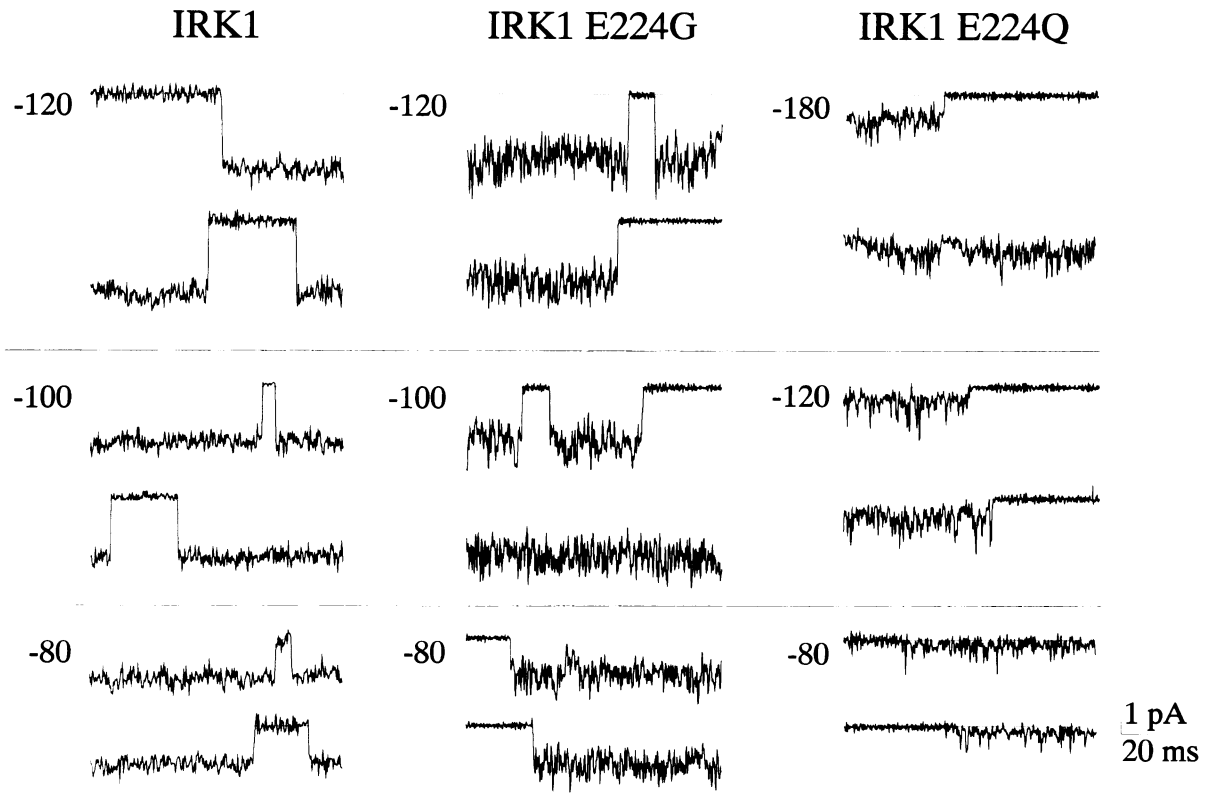

Fig. 6. Single-channel properties of IRK1 E244 mutants. Single channel currents from the indicated mutants were recorded in the cell-attached configuration. Pipette and bath solutions were K^+-Ringer and iso-K^+ respectively. Test potentials are indicated. Sampling: 5 kHz; filter: 1 kHz.

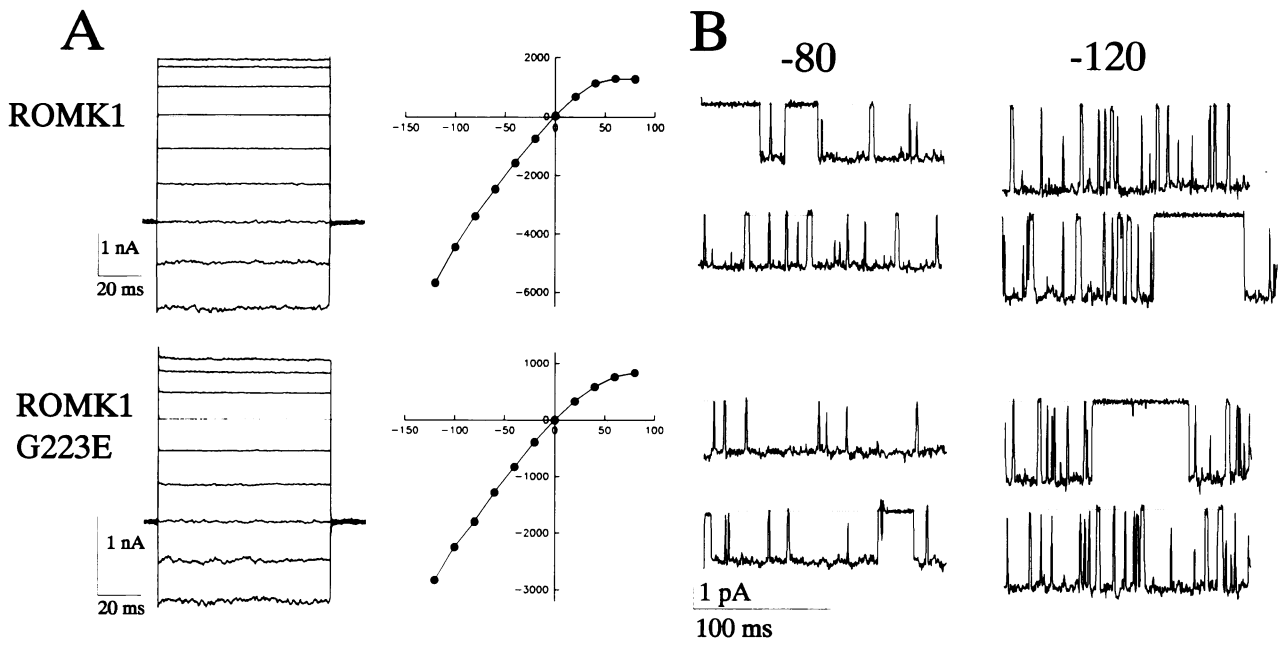

Fig. 7. Similar macroscopic and single channel properties of the ROMK1 and ROMK1 G223E mutant. (**A**) Unsubtracted cell-attached macropatch recordings from *Xenopus* oocytes injected with ROMK1 and ROMK1 G223E cRNAs. Holding potential: –60 mV. Test pulses from –100 mV to +60 mV, in 20 mV steps; return potential: –60 mV. Also shown is the relationship of the steady-state current (measured at the end of the depolarizing pulses) to voltage. (**B**) Cell-attached single-channel currents recorded from oocytes injected with the cRNA encoding for ROMK1 and ROMK1 G223E channels. Pipette and bath solutions were K^+-Ringer and iso-K^+ respectively. Test potentials are indicated. Sampling: 5 kHz; filter: 1 kHz.

channel to concentrate K^+ ions (Lu and MacKinnon, 1994).

In the inside-out configuration, the addition of 100 μM SPD to the internal side of the patch caused <5% block of the outward currents at +40 mV (n = 4), and the K_d for SPD was estimated to be higher than 500 μM (Table I). This low intrinsic affinity for SPD of the double IRK1 mutant closely resembles the low affinity of ROMK1 for

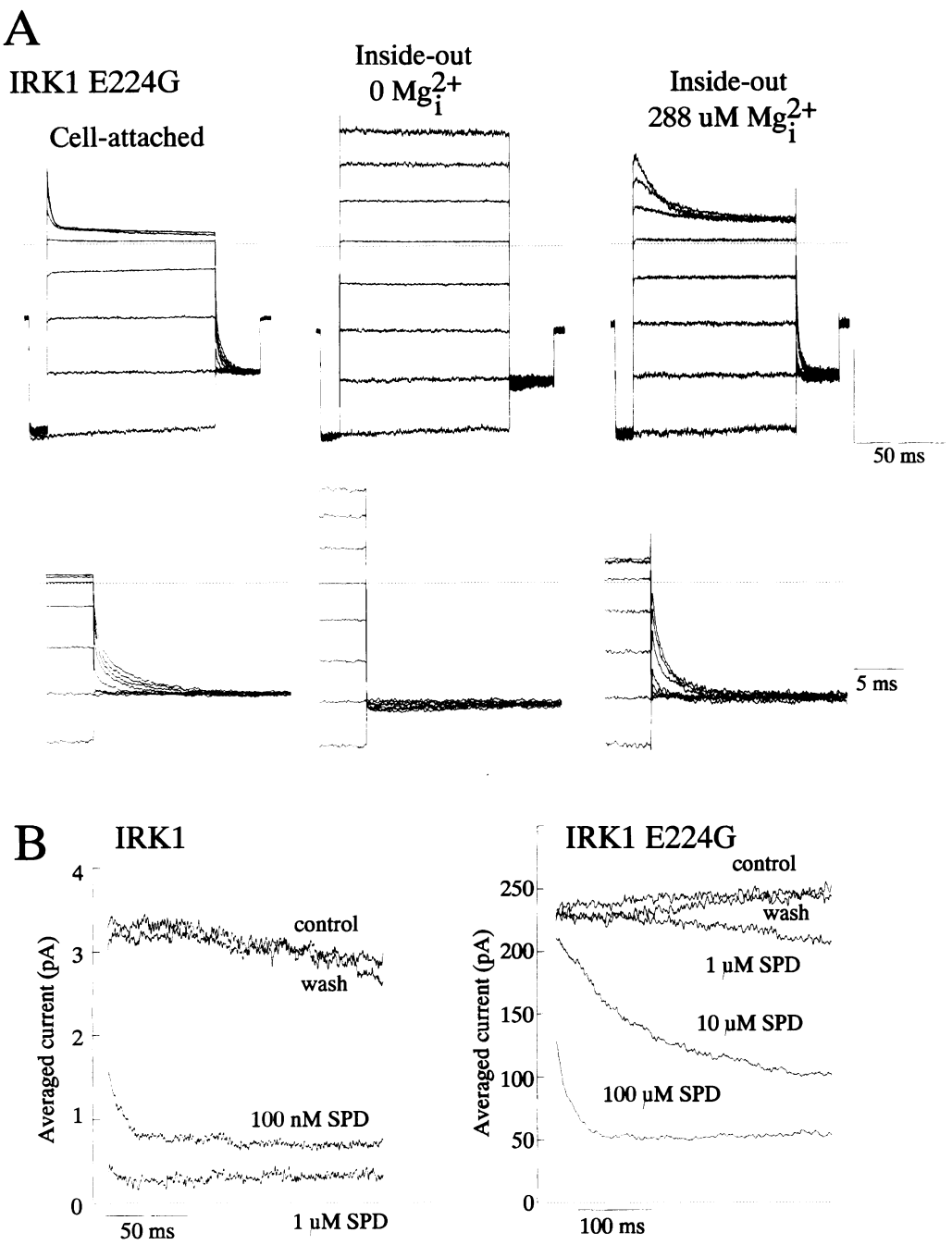

Fig. 8. Reduced affinity for internal Mg^{2+} and SPD in IRK1 E224G channels. (**A**) Unsubtracted macropatch recordings from *Xenopus* oocytes injected with IRK1 E224G cRNA, recorded in the cell-attached configuration, after patch excision in a Mg^{2+}-free and SPD-free solution, and after patch exposure to 288 µM internal Mg^{2+}. Holding potential: –40 mV; pre-pulse potential: –80 mV; test pulses from –80 mV to +60 mV, in 20 mV steps; return potential: –60 mV. The current traces recorded upon return to –60 mV after the depolarizing steps are also shown on an expanded time scale. The vertical scale bar is 500 pA for the cell-attached, 342 pA for the inside-out zero Mg^{2+}, and 253 pA for the 288 µM internal Mg^{2+}: this decrease is due to fast channel rundown in the inside-out configuration. Bath and pipette solution are identical to those described in the legend to Figure 3, except that in the bath solution 10 mM EGTA substituted 10 mM EDTA. The desired concentration of free Mg^{2+} was achieved as described (Fabiato and Fabiato, 1979; Taglialatela *et al.*, 1994). (**B**) Averaged IRK1 (left) and IRK1 E224G (right) single-channel records from multichannel patches (4–6 channels in IRK1; 200–1000 channels in IRK1 E224G) recorded in the inside-out configuration in control solution, upon exposure to the indicated concentrations of SPD, and upon SPD washout. Test potential: +40 mV. Pipette and bath solutions were iso-K^+ and K^+-Ringer respectively.

this organic cation (Table I). As in the case of the single IRK1 E224 mutant, similar permeation and blocking properties were observed in a double mutant in which the C-terminal negatively charged site was neutralized with a more conservative glutamine substitution (IRK1 D172N+ E224Q) (Table I).

Discussion

Exchange of the C-terminal region between the strong inward rectifier IRK1 and the weak inward rectifier ROMK1 generated a channel (ROMK/IRK CHM C or CHM C_1–C_5) which acquired strong rectification

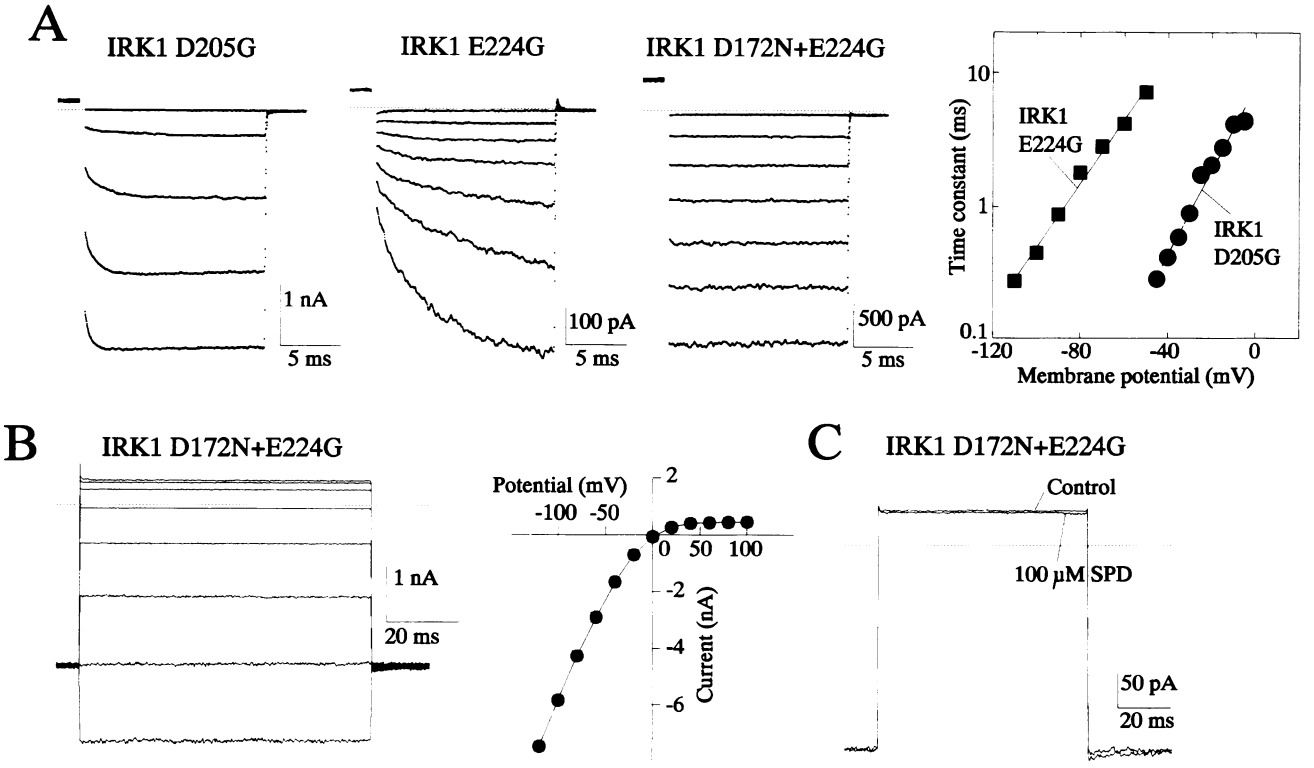

Fig. 9. Functional properties of the IRK1 D172N+E224G double mutant. (**A**) Unsubtracted cell-attached macropatch recordings from *Xenopus* oocytes injected with IRK1 D205G, IRK1 E224G and IRK1 D172N+E224G cRNAs. Holding potential: –60 mV; depolarizing step: +40 mV; hyperpolarizing pulses: from 0 to –40 mV (IRK1 D205G) or to –60 mV (IRK1 E224G and IRK1 D172N+E224G), in –10 mV steps; return potential: 0 mV. Only the current responses during the last 2 ms of the depolarizing steps, the hyperpolarizing pulses and the first 3 ms of the return pulses are reported. The first 500 μs of the capacitive artifact recorded during the hyperpolarizing pulses have been blanked (Ficker *et al.*, 1994). The right panel reports the time constants for current activation during the hyperpolarizing pulses measured from monoexponential fits (Wible *et al.*, 1994). The data are from one cell for each mutant, representative of six each. (**B**) Unsubtracted inside-out macropatch recordings from IRK1 D172N+E224G channels in Mg^{2+}- and PA-free solution. Holding potential: –60 mV; depolarizing step: from –80 mV to +60 mV in 20 mV steps; return potential: –60 mV. Also reported is the current to voltage relationship measured at the end of the depolarizing pulses. (**C**) Unsubtracted inside-out macropatch recordings from *Xenopus* oocytes expressing IRK1 D172N+E224G channels in control solution and after patch exposure to 100 μM SPD. Holding potential: –60 mV; depolarizing step: +40 mV; return potential: –60 mV. In all panels, pipette and bath solutions were K^+-Ringer and iso-K^+ respectively.

(Taglialatela *et al.*, 1994). This rectification involved an increased affinity for internal cations, particularly Mg^{2+} and polyamines. Neither blocker produced any time-dependence in inward current activation of the C-terminus chimeric channel, suggesting fast rates of interaction with the open channel. By subdividing the C-terminus into shorter segments, we have now demonstrated that residue(s) in the IRK1 C-terminus conferring strong inward rectification are located in the C_1 region, a 72 amino acid region past the second putative transmembrane domain. Single-point mutations at the four non-conservative charge substitutions between IRK1 and ROMK1 (positions 191, 205, 224 and 249), have identified the residue at position 224 in IRK1 as the crucial molecular determinant of this phenomenon. In fact, mutation E224G in IRK1 drastically reduced inward rectification. In this mutant, internal Mg^{2+} and SPD affinities were reduced by at least 10- and 10^3-fold, respectively, suggesting that this position is involved in the formation of the binding pocket for these internal cations. The reduced ability of internal Mg^{2+} and SPD in blocking the IRK1 E224G channel is responsible for the decreased inward rectification of this channel. Since both Mg^{2+} and SPD binding are strongly voltage-dependent (Matsuda *et al.*, 1987; Vandenberg, 1987; Ishihara *et al.*, 1989; Lu and MacKinnon, 1994; Wible *et al.*, 1994), it seems likely that the binding sites for these molecules are located within the membrane electric field. Furthermore, the fast rates of interaction of these blockers with the open ROMK1/IRK1 CHM C_1–C_5 channels seems strongly supportive of a direct interaction between the blockers and the channel protein, possibly occurring at the level of the ion conduction pathway. The decreased inward rectification observed in the IRK1 E224G mutant when compared with wild-type IRK1 suggests, therefore, that the E224 residue is located in the ion conduction pathway. This conclusion is supported by the profound alteration in the apparent K^+ conductance demonstrated by single-channel recordings in the IRK1 E224G mutant. In fact, the long openings characteristic of IRK1 channels were extremely flickery in the IRK1 E224G mutants, with a marked increase in the open channel noise. Even more marked alterations were observed when a more conservative E224Q substitution was made at this position. In addition, since the charge at E224 is conserved among strong inward rectifiers but absent in weak inward rectifiers (Wible *et al.*, 1995), it appears that this residue is a crucial determinant of the unique permeation and blocking properties of IRKs.

The simultaneous reduction of internal Mg^{2+} and SPD binding in the IRK1 E224G mutation stands in sharp

contrast to the results obtained at position D172 in the putative second transmembrane domain (M_2) of IRK1. The IRK1 D172N mutant only slightly affected the binding of internal Mg^{2+} (Wible *et al.*, 1994), but did cause a 30-fold reduction in SPD affinity (Ficker *et al.*, 1994). The ability of the IRK1 D172 position to discriminate between Mg^{2+} and SPD explains why the IRK1 D172N mutant lacked SPD-induced time-dependence while retaining strong inward rectification.

The different contribution in IRK1 of M_2 position 172 and C-terminus position 224 to internal Mg^{2+} and PA binding suggests that SPD is best retained at position 172 when properly bound to the C-terminal E224 site. Mg^{2+}, on the other hand, interacts strongly and preferentially with the C-terminal E224 residue. Thus two sites, one in M_2 and the other in the C-terminus, contribute to the binding of these cations in IRK1. However, in ROMK1, the corresponding C-terminal site is lacking and could not be reconstituted by the G223E mutation, suggesting differences in the contribution of the C-terminus sites in the molecular architecture between IRK1 and ROMK1 pores.

The strong cooperativity for cation binding occurring between the negatively charged residues at position 172 and 224 in IRK1 is further demonstrated by the fact that a double mutant IRK1 D172N+E224G, in which both sites are neutralized, decreased SPD binding more markedly than the two single mutants separately. This result suggests that these two sites influence cation binding simultaneously and independently, as recently hypothesized (Yang *et al.*, 1995).

In conclusion, we have presently identified a negatively charged residue (E224) in the C-terminal region of IRK1 which appears to play a crucial role in controlling ion conduction and pore block. The strong contribution of E224 to the pore properties of IRK1 would suggest that this residue is membrane-associated, in contrast to the currently proposed topological map for this channel. The identification of this site, together with future work aimed to clarify its interaction with other sites in the channel, particularly position 172, is an important step toward the definiton of the molecular mechanisms by which inward rectification is achieved.

Materials and methods

Standard recombinant DNA techniques and site-directed mutagenesis

Standard methods of plasmid DNA preparation and DNA sequencing were used (Sambrook *et al.*, 1989). IRK1 cDNA in the vector pcDNA1 was kindly provided by Dr L.Jan. ROMK1 cDNA was obtained by reverse transcriptase polymerase chain reaction (RT-PCR) using rat kidney total RNA as template (Wible *et al.*, 1994). PCR overlap extension was used for engineering ROMK1/IRK1 chimeric cDNA constructs (Horton *et al.*, 1989), as well as for introducing single point mutations in ROMK1 and IRK1 cDNAs (Ho *et al.*, 1989), as previously described (Taglialatela *et al.*, 1994). The mutant constructs were subcloned as *ApaI–EcoRI* fragments into a modified PCRII vector (Invitrogen, San Diego, CA) containing a portion of the rat DRK1 3′ untranslated poly(A)$^+$ tail region. cRNAs for injection into *Xenopus* oocytes were prepared using the mMESSAGE mMACHINE kit (Ambion) with T7 RNA polymerase following linearization of the plasmids with *BamH1* or *NotI*.

In vitro transcription of the mRNAs and oocyte injection

Stage V–VI *Xenopus* oocytes were surgically removed from anesthesized frogs (0.1% tricaine). Oocyte defolliculation was achieved by exposing the oocytes to collagenase (2 mg/ml, 1.5 h) in OR2 solution (in mM): 82.5 NaCl, 2.5 KCl, 1 $MgCl_2$, 5 HEPES, (+ 100 μg/ml gentamicin), pH 7.6. Following this, oocytes were incubated at 19°C in SOS solution (in mM): 100 NaCl, 2 KCl, 1.8 $CaCl_2$, 1 $MgCl_2$, 5 HEPES, 2.5 Pyruvic acid (+ 100 μg/ml gentamicin), pH 7.6. One day after isolation, defolliculated oocytes were injected with 46 nl of 1–100 ng/μl of cRNA solutions in 0.1 M KCl. For single-channel recording, the vitelline membrane was manually removed.

Electrophysiology

Whole-cell measurements. Two to five days after the injection, the oocytes were voltage-clamped using a commercial two-electrode voltage clamp amplifier (Dagan 8500, Dagan Corp.). Current and voltage electrodes were filled with 3 M KCl, 10 mM HEPES (pH 7.4; ~1 MΩ resistance). The bath solutions were (in mM): low K^+-MES (120 *N*-methyl-D-glucamine, 120 MES, 2.5 KOH, 2 $Mg(OH)_2$ and 10 HEPES, pH 7.4), and high K^+-MES (22.5 *N*-methyl-D-glucamine, 122.5 MES, 100 KOH, 2 $MgOH_2$ and 10 HEPES, pH 7.4). The PClamp system (Axon Instruments) was used for the generation of the voltage pulse protocols and for data acquisition. No leak subtraction procedure was used.

Macropatch currents. Macropatch currents from *Xenopus* oocytes were recorded using the giant patch technique (Hilgemann, 1989). We modified the original technique in such a way that no vaseline or other sealant material was used. The diameter of the patch pipette was between 15 and 20 μm (between 0.2 and 0.5 MΩ resistance); the seal resistance was usually >10 GΩ. The pipette tips were Sylgard-coated (Dow-Corning, Midland, MI) to reduce the glass capacitance. The pipette solution was K^+-Ringer (in mM: 100 KCl, 2 $MgCl_2$, 10 HEPES, pH 7.3), while the depolarizing bath solution was iso-K^+ (in mM: 100 KCl, 10 EDTA, 10 HEPES, pH 7.3). When necessary, $MgCl_2$ or Mg-ATP was added to the bath solution to give calculated concentrations of free Mg^{2+} ions (Fabiato and Fabiato, 1979). Holding and test potentials applied to the membrane patch are reported as conventional absolute intracellular potentials assuming that the oocyte resting potential was zeroed by the bathing solution.

Single channel currents. Single channel currents were recorded from cell-attached and inside-out membrane patches using oocytes dissected free of the vitelline envelope and micropipettes of 2–5 MΩ resistance that were fire-polished and Sylgard-coated. The pipette and bath solutions were the same as those utilized for macropatch recordings. Data were low-pass filtered at 1 kHz (–3 dB, 4-pole Bessel filter) prior to digitization at 5 kHz. Channels were activated with rectangular test pulses from negative holding potentials (–80 mV to –120 mV). Current records were corrected for capacitative and leakage currents by subtracting the smoothed average of records lacking channel activity ('null traces'). Data were analyzed as described (Kirsch *et al.*, 1992). Both whole-cell and single-channel experiments were performed at room temperature (22–24°C) in a recording chamber which was continuously superfused with bath solution at a rate of 2 ml/min.

Acknowledgements

We thank Dr L.Jan for providing the IRK1 clone; Mr R.Cockrell for injecting and handling oocytes; T.Affini and S.Dou for expert molecular biology support. This work was supported in part by National Institutes of Health grants to A.M.Brown, grants from the AHA-Texas Affiliate (94G-218) and Telethon (748) to M.Taglialatela and a grant from the A.von Humboldt Foundation to E.Ficker.

References

Dascal,N. *et al.* (1993) Atrial G protein-activated K^+ channel:expression, cloning and molecular properties. *Proc. Natl Acad. Sci. USA*, **90**, 10235–10239.

Fabiato,A. and Fabiato,F. (1979) Calculator programs for computing the composition of the solutions containing multiple metals and ligands used for experiments in skinned muscle cells. *J. Physiol., Paris*, **74**, 463–505.

Fakler,B., Brandle,U., Bond,C., Glowatzki,E., Konig,C., Adelman,J.P., Zenner,H.-P. and Ruppersberg,J.P. (1994) A structural determinant of differential sensitivity of cloned inward rectifier K^+ channels to intracellular spermine. *FEBS Lett.*, **356**, 199–203.

Fakler,B., Brandle,U., Glowatzki,E., Weidemann,S., Zenner,H.-P. and Ruppersberg,J.P. (1995) Strong voltage-dependent inward rectification

of inward rectifier K^+ channels is caused by intracellular spermine. *Cell*, **80**, 149–154.

Ficker,E., Taglialatela,M., Wible,A.M., Henley,C.M. and Brown,A.M. (1994) Spermine and spermidine as gating molecules for inward rectifier K^+ channels. *Science*, **266**, 1068–1972.

Hilgemann,D.W. (1989) Giant excised cardiac sarcolemmal membrane patches: sodium and sodium–calcium exchange currents. *Pflügers Arch.*, **415**, 247–249.

Hille,B. (1992) *Ionic Channels of Excitable Membranes*. 2nd edn. Sinauer Ass., Sunderland, MA.

Ho,K., Nichols,C.G., Lederer,W.J., Lytton,J., Vassilev,P.M., Kanazirska, M.V. and Hebert,S.C. (1993) Cloning and expression of an inwardly rectifying ATP-regulated potassium channel. *Nature*, **362**, 31–38.

Ho,S.N., Hunt,H.D., Horton,R.M., Pullen,J.K. and Pease,L.R. (1989) Site-directed mutagenesis by overlap extension using the polymerase chain reaction. *Gene*, **77**, 51–59.

Horton,R.M., Hunt,H.D., Ho,S.N., Pullen,J.K. and Pease,L.R. (1989) Engineering hybrid genes without the use of restriction enzymes: gene splicing by overlap extension. *Gene*, **77**, 61–68.

Ishihara,K., Mitsuye,T., Noma,A. and Takano,M. (1989) The Mg^{2+} block and intrinsic gating underlying inward rectification of the K^+ current in guinea-pig cardiac myocytes. *J. Physiol., Lond.*, **419**, 297–320.

Kirsch,G.E., Drewe, J.A., Taglialatela,M., DeBiasi,M., Hartmann,H.A. and Brown,A.M. (1992) A single non-polar residue in the deep pores of related K^+ channels acts as a K^+:Rb^+ conductance switch. *Biophys. J.*, **62**, 136–144.

Kubo,Y., Baldwin,T., Jan,Y.N. and Jan,L.Y. (1993a) Primary structure and functional expression of a mouse inward rectifier potassium channel. *Nature*, **362**, 127–133.

Kubo,Y., Reuveny,E., Slesinger,P.A., Jan,Y.N. and Jan,L.Y. (1993b) Primary structure and functional expression of a rat G-protein-coupled muscarinic potassium channel. *Nature*, **364**, 802–806.

Kyte,J. and Doolittle,R.F. (1982) A simple method for displaying the hydropathic character of a protein. *J. Mol. Biol.*, **157**, 105–132.

Lopatin,A.N., Makhina,E.N. and Nichols,C.E. (1994) Potassium channel block by cytoplasmic polyamines as the mechanism of intrinsic rectification. *Nature*, **372**, 366–369.

Lu,Z. and MacKinnon,R. (1994) Electrostatic tuning of Mg^{2+} affinity in an inward-rectifier K^+ channel. *Nature*, **371**, 243–246.

Matsuda,H., Saigusa,A. and Irisawa,I. (1987) Ohmic conductance through the inwardly rectifying K channel and blocking by internal Mg^{2+}. *Nature*, **325**, 156–159.

Sambrook,J., Fritsch,E.F. and Maniatis,T. (1989) *Molecular Cloning. A Laboratory Manual*. 2nd edn. Cold Spring Harbor Laboratory Press, Cold Spring Harbor, NY.

Silver,M.R. and DeCoursey,T.E. (1990) Intrinsic gating of inward rectifier in bovine pulmonary artery endothelial cells in the presence or absence of internal Mg^{2+}. *J. Gen. Physiol.*, **96**, 109–133.

Stanfield,P.R., Davies,N.W., Shelton,I.A, Sutcliffe,M.J., Khan,I.A., Brammar,W.J. and Conley,E.C. (1994) A single aspartate residue is involved in both intrinsic gating and blockage by Mg^{2+} of the inward rectifier IRK1. *J. Physiol., Lond.*, **478**, 1–6.

Taglialatela,M. Wible,B.A., Caporaso,R. and Brown,A.M. (1994) Specification of pore properties by the carboxyl terminus of inwardly rectifying K^+ channels. *Science*, **264**, 844–847.

Vandenberg,C.A. (1987) Inward rectification in cardiac ventricular cells depends on internal magnesium ions. *Proc. Natl Acad. Sci. USA*, **84**, 2560–2564.

Wible,B.A., Taglialatela,M., Ficker,E. and Brown,A.M. (1994) Gating of inwardly rectifying K^+ channels localized to a single negatively charged residue. *Nature*, **371**, 246–249.

Wible,B.A., DeBiasi,M., Majumder,K., Taglialatela,M. and Brown,A.M. (1995) Cloning and functional expression of an inwardly-rectifying K^+ channel from human atrium. *Circ. Res.*, **76**, 343–350.

Yang,J., Jan,Y.N. and Jan,L.Y. (1995) Control of rectification and permeation by residues in two distinct domains in an inwardly rectifying K^+ channel. *Neuron*, **14**: 1047–1054.

Received on May 17, 1995; revised on July 28, 1995